

# Superfluid Dynamics within Time-Dependent Density Functional Theory

K. Sekizawa<sup>1,2</sup>, A.E. Makowski<sup>3</sup>, A. Barresi<sup>3</sup>, P. Magierski<sup>3,4</sup>, G. Wlazłowski<sup>3,4</sup>, D.Z. Pećak<sup>3</sup>, M.J. Tylutki<sup>3</sup>,  
B. Tüzemen<sup>3</sup>, K. Kobuszewski<sup>3</sup>, A.M.A. Boulet<sup>3</sup>, W. Kragiel<sup>3</sup>, A. Bulgac<sup>4</sup>

<sup>1</sup>Department of Physics, Tokyo Institute of Technology, Japan

<sup>2</sup>Center for Computational Sciences, University of Tsukuba, Japan

<sup>3</sup>Faculty of Physics, Warsaw University of Technology, Poland

<sup>4</sup>Department of Physics, University of Washington, USA

## Method

### We employ Time-Dependent Superfluid Local Density Approximation: TDSLDA

To describe superfluid dynamics in strongly-correlated Fermionic systems, we use **Time-Dependent Density Functional Theory (TDDFT) extended to superfluid systems, known as TDSLDA** [1]. We solve it in 3D uniform grids without symmetry restrictions. Since it requires to solve a huge number ( $10^4$ - $10^6$ ) of 3D, complex, non-linear, coupled PDEs, we do need a supercomputer. With local treatment of pairing, the equations could be solved efficiently on **GPUs**: each thread takes care of each lattice point. With the usage of supercomputers, it has been successfully applied to, e.g., collisions of two superfluid nuclei [2] as well as vortex-nucleus dynamics in the inner crust of neutron stars [3].

#### TDSLDA: TDDFT with local treatment of pairing

Kohn-Sham scheme is extended for non-interacting quasiparticles

► TDSLDA equations (formally equivalent to TDHFB or TD-BdG equations)

$$i\hbar \frac{\partial}{\partial t} \begin{pmatrix} u_{k,\uparrow}(\mathbf{r}, t) \\ u_{k,\downarrow}(\mathbf{r}, t) \\ v_{k,\uparrow}(\mathbf{r}, t) \\ v_{k,\downarrow}(\mathbf{r}, t) \end{pmatrix} = \begin{pmatrix} h_{\uparrow\uparrow}(\mathbf{r}, t) & h_{\uparrow\downarrow}(\mathbf{r}, t) & 0 & \Delta(\mathbf{r}, t) \\ h_{\downarrow\uparrow}(\mathbf{r}, t) & h_{\downarrow\downarrow}(\mathbf{r}, t) & -\Delta(\mathbf{r}, t) & 0 \\ 0 & -\Delta^*(\mathbf{r}, t) & -h_{\uparrow\uparrow}^*(\mathbf{r}, t) & -h_{\uparrow\downarrow}^*(\mathbf{r}, t) \\ \Delta^*(\mathbf{r}, t) & 0 & -h_{\downarrow\uparrow}^*(\mathbf{r}, t) & -h_{\downarrow\downarrow}^*(\mathbf{r}, t) \end{pmatrix} \begin{pmatrix} u_{k,\uparrow}(\mathbf{r}, t) \\ u_{k,\downarrow}(\mathbf{r}, t) \\ v_{k,\uparrow}(\mathbf{r}, t) \\ v_{k,\downarrow}(\mathbf{r}, t) \end{pmatrix}$$

$$h_{\sigma} = \frac{\delta E}{\delta n_{\sigma}} : \text{s.p. Hamiltonian}$$

$$\Delta = -\frac{\delta E}{\delta \nu^*} : \text{pairing field}$$

$$n_{\sigma}(\mathbf{r}, t) = \sum_{E_k < E_c} |v_{k,\sigma}(\mathbf{r}, t)|^2 : \text{number density}$$

$$\nu(\mathbf{r}, t) = \sum_{E_k < E_c} u_{k,\uparrow}(\mathbf{r}, t)v_{k,\downarrow}^*(\mathbf{r}, t) : \text{anomalous density}$$

$$\mathbf{j}_{\sigma}(\mathbf{r}, t) = \hbar \sum_{E_k < E_c} \text{Im}[v_{k,\sigma}^*(\mathbf{r}, t)\nabla v_{k,\sigma}(\mathbf{r}, t)] : \text{current}$$

**A large number ( $10^4$ - $10^6$ ) of 3D coupled non-linear PDEs have to be solved!!**  
# of qp orbitals ~ # of grid points

[1] A. Bulgac, Ann. Rev. Nucl. Part. Sci. **63**, 97 (2013);

P. Magierski, Fron. Nucl. Part. Phys. **2**, 57-71 (Bentham Science Publishers 2019).

[2] P. Magierski, K. Sekizawa, and G. Wlazłowski, Phys. Rev. Lett. **119**, 042501 (2017).

[3] G. Wlazłowski, K. Sekizawa, P. Magierski, et al., Phys. Rev. Lett. **117**, 232701 (2016).

## Results (1/2)

### We found rapid increases of pairing in fusing magic nuclei

Pairing correlations (superfluidity and superconductivity) in nuclear systems are one of the best-known characteristics of **non-magic (open shell)** atomic nuclei. **Magic nuclei**, on the other hand, having **closed shells** of nucleon orbitals (akin to noble gases of atoms), are known to exhibit vanishing pairing due to the shell gap. It has thus been believed that theories neglecting pairing correlations are enough to describe the collisions of magic nuclei as well as their ground state properties. We have found, based on fully microscopic simulations taking into account pairing correlations, that **the pairing correlations may be important even in collisions of two magic nuclei**.

Within this project, we have investigated collisions of several magic nuclei which merge into sufficiently long-lived compound systems:  $^{40}\text{Ca}+^{208}\text{Pb}$ ,  $^{90}\text{Zr}+^{90}\text{Zr}$ ,  $^{90}\text{Zr}+^{132}\text{Sn}$ ,  $^{48}\text{Ca}+^{208}\text{Pb}$  and  $^{56}\text{Ni}+^{208}\text{Pb}$ . From the results, we have found that the pairing correlations are dynamically induced after the collisions. The enhancement of pairing correlations is a generic feature observed in all systems examined, which occurs during the collision **as a result of rapid change of the density of states in the compound system**. The instability is indicated by the exponential growth of the magnitude of pairing field within time scales of 1000 fm/c ( $\sim 3 \times 10^{21}$  sec). Surprisingly it is weakly dependent on the collision energy, but is sensitive to the angular momentum transfer to the system [see [Figs. 1 and 2](#)]. The effect resembles the Higgs mechanism triggered by nuclear collision. A paper is in preparation.

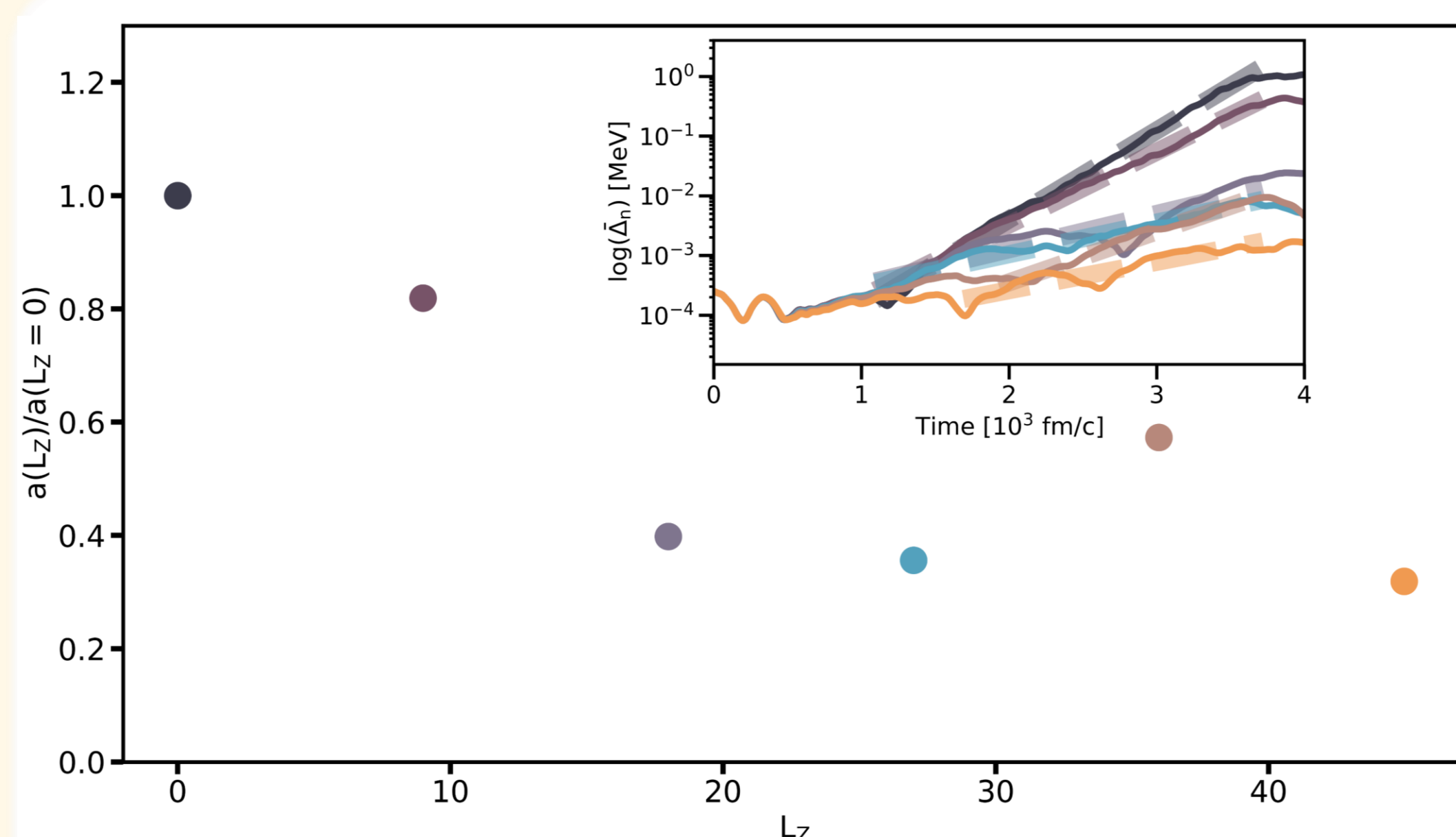


Fig. 2: The normalized slope for the increasing average neutron pairing gap  $\Delta_n$  (cf. dashed lines in the inset) in the  $^{40}\text{Ca}+^{208}\text{Pb}$  reaction at  $E_{\text{cm}}=200$  MeV as a function of the angular momentum,  $L_z = b\sqrt{2\mu E_{\text{cm}}}/\hbar$  ( $b$  is the impact parameter). In the inset, evolution of  $\Delta_n$  is presented as a function of time in logarithmic scale.

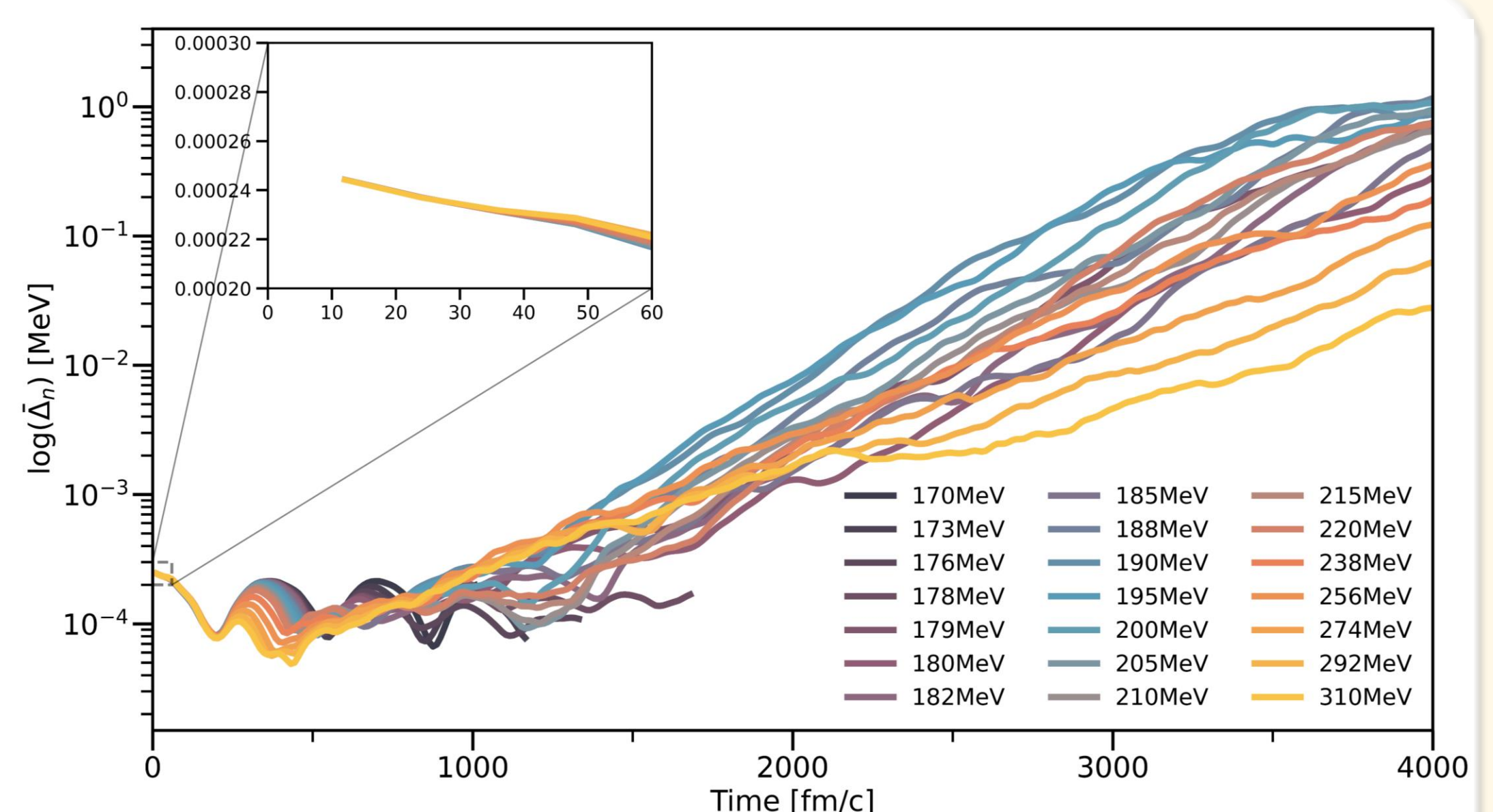


Fig. 3: Evolution of the average neutron pairing gap  $\Delta_n$  as a function of time for the  $^{40}\text{Ca}+^{208}\text{Pb}$  reaction at various collision energies in logarithmic scale. The inset presents the first time steps after the nuclei are accelerated. This figure illustrates the rapid increase of pairing during collisions.



[Quadrupole collisions] Pre-print: <https://arxiv.org/abs/2207.00870>

We have examined collisions of vortex pairs in trapped gases of fermions in different interaction regimes. We show the relation between density of bound states inside vortex cores upon collision and temperature of the system in both unitary Fermi gas and BCS regime. As posited by Silaev [Phys. Rev. Lett. **108**, 045303 (2012)], leakage of bound states is shown to be directly related to dissipation, which can be measured by tracking vortex trajectories.

We have found that results at zero temperature show a different behavior from finite temperature experiments realized in Kwon *et al.* [Nature (London) **600**, 64 (2021)]. At higher temperatures, thermal effects significantly affect the observed dynamics, pointing to the crucial role of mutual friction with normal component. The dissipative mechanism via excitations of the vortex core emerges as of secondary importance. For details of the results, see [Fig. 3](#).

[Dipole propagation in polarized systems]

We have examined the dynamics of a single vortex pair propagating in a unitary spin-imbanced Fermi gas. Additionally, we introduce inhomogeneities in the spatial distribution of polarization, in order to explore the interactions between vortex dipoles and ferrons. Moreover, attempts of scattering length quenching are being explored, in order to explore the behavior of Andreev states, vortex structure and propagation in the presence of induced Higgs modes.

At the preliminary stage, we found that in polarized systems the dynamics of the dipole is impacted by its structure. In the case of polarization localized in clusters (ferrons), the formation of a Jones-Robertson soliton precedes linear propagation. Interaction with ferrons requires further investigation. In the case of uniform polarization and induced Higgs modes, the dipole structure is not impacted until the Higgs mode decays, which results in the annihilation of the vortex cores. Further investigation is required. Some illustrative examples are presented in [Fig. 4](#).

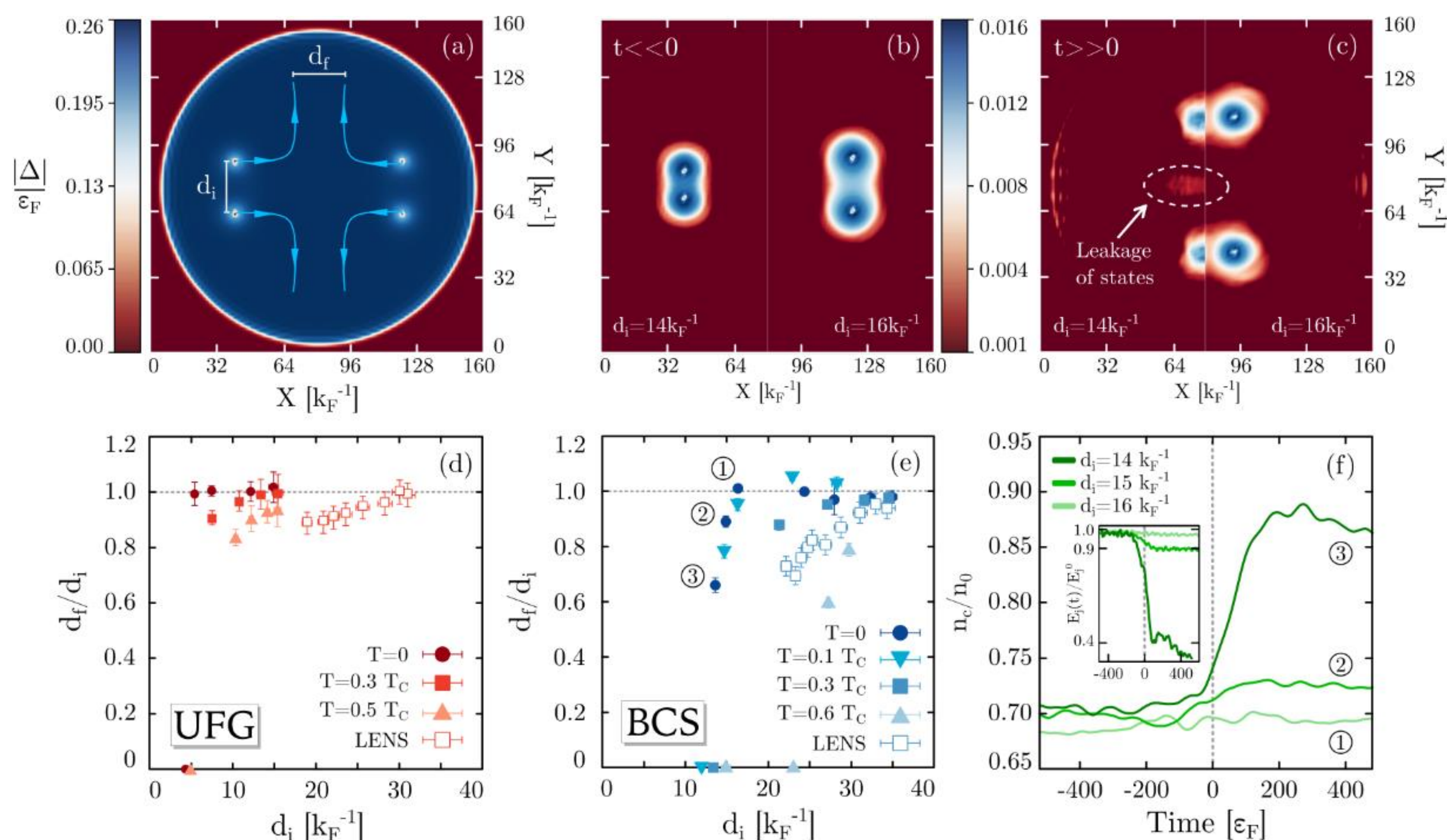


Fig. 3: (a): Initial configuration (BCS regime with  $a_s k_F = -1$ ) showing distribution of the order parameter  $\Delta$ . During dynamics, vortices are moving along blue lines. Distance between vortices before and after collision is indicated by  $d_i$  and  $d_f$ , respectively. (b) and (c): Spatial distribution of density arising from the Andreev states, before ( $t \ll 0$ ) and after collision ( $t \gg 0$ ). Boxes are divided in half, corresponding to different initial distances of vortices in the BCS regime. (d) and (e): Relative decrease in distance between vortices in the case of two dipoles colliding head-on in UFG and BCS regimes at various temperatures. Results of LENS are included. (f): Core density, normalized to the bulk density, as a function of time for zero temperature BCS runs.  $t=0$  indicates collision moment. Inset: flow energy  $E_f$  as a function of time, normalized to its initial value.

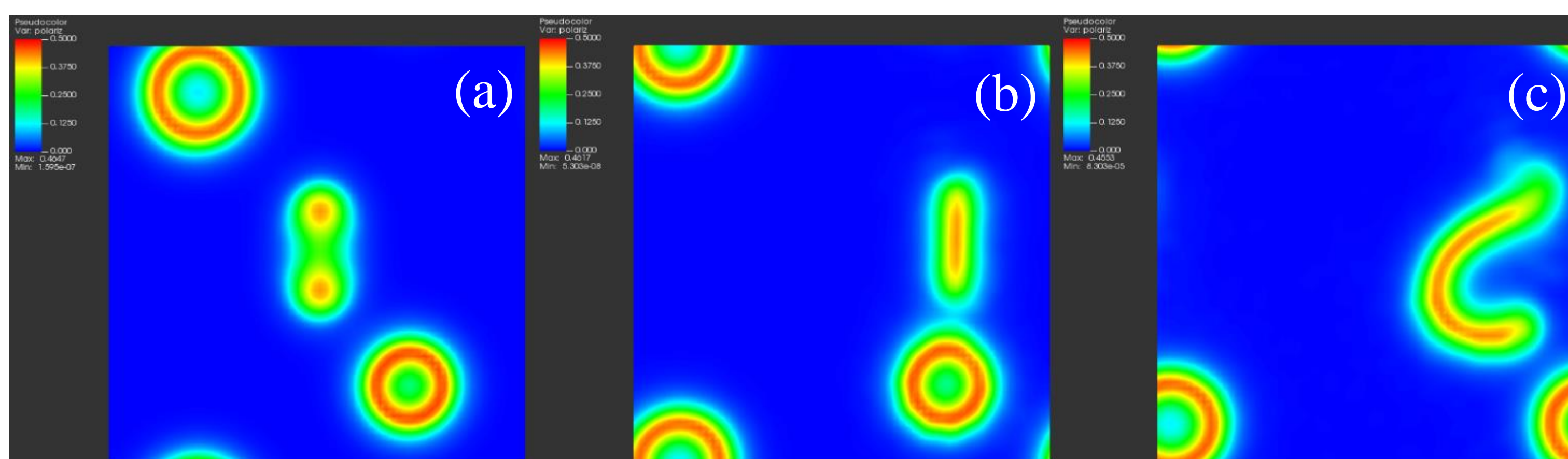


Fig. 4: Polarization at various times of the dipole propagation. (a)  $t=0$ , the vortex cores are well separated. (b)  $t=t_1 \gg 0$ , the cores merge, forming a Jones-Robertson soliton that propagates in the direction given by the initial currents. (c)  $t=t_2 > t_1$ , the soliton interacts with ferrons, which become unstable.